On estimating length fluctuations of glaciers caused by changes in climatic forcing

G. J.-M. C. Leysinger Vieli[1] and G. H. Gudmundsson[2]

Section of Glaciology, Laboratory of Hydraulics, Hydrology and Glaciology/Eidgenössische Technische Hochschule Zürich, Zürich, Switzerland

Received 7 February 2003; revised 13 November 2003; accepted 28 November 2003; published 13 February 2004.

[1] The reaction of alpine glaciers to shifts in the equilibrium line altitude (ELA) is calculated by using a two-dimensional numerical model to solve the full equations for the velocity and stress fields (full-system model) in the absence of basal motion. Rates of advance and retreat of the snout of typically sized alpine glaciers are found to be insensitive to the details of the flow at the snout, even when the glaciers are far from steady state. A comparison of results obtained with a full-system model and a shallow ice approximation (SIA) model yields no significant differences in advance or retreat rates. This assumption has been implicitly made in numerous previous climatic studies and is here shown to be well justified. Using a realistic mass balance altitude feedback, only slight model-dependent changes in steady state lengths are found. The relative importance of mass balance and glacier dynamics for the transient response of alpine glaciers to changes in the ELA is given a precise meaning by determining the model-dependent additional shifts in ELA needed for the SIA and the full-system models to produce identical changes in length. For alpine glaciers, these additional shifts in ELA are on the order of 10 m, which is within the error range of ELA estimates. It follows that at least in the absence of significant basal motion, there is no need to include the effects of horizontal stresses when calculating the reaction of alpine glaciers to climatic changes. Attention should focus on accurate determination of the mass balance distribution and model tuning to give realistic ice thickness distributions. *INDEX TERMS:* 1620 Global Change: Climate dynamics (3309); 1827 Hydrology: Glaciology (1863); 1823 Hydrology: Frozen ground; 3210 Mathematical Geophysics: Modeling; 3220 Mathematical Geophysics: Nonlinear dynamics; *KEYWORDS:* glacier dynamics, higher-order model, model-model comparison, length fluctuations, glacier response times, rock glaciers

Citation: Leysinger Vieli, G. J.-M. C., and G. H. Gudmundsson (2004), On estimating length fluctuations of glaciers caused by changes in climatic forcing, *J. Geophys. Res.*, *109*, F01007, doi:10.1029/2003JF000027.

1. Introduction

[2] There is considerable interest in retrieving information on past climatic history using records of glacier fluctuations and in determining future changes in size and distribution of glaciers caused by possible future global climate change [e.g., *Haeberli and Beniston*, 1998; *Oerlemans*, 2001]. For the transient evolution of large ice masses to be calculated, both the mass balance variation in space and time and the mechanics of glacier flow must be accounted for. The question arises as to what level of detail the mechanics of ice flow must be described for the purpose of calculating climate-related length changes over timescales longer than a few years.

[3] Here we address this question by comparing two numerical models of the retreat and advance of typically sized alpine glaciers: a two-dimensional model including all terms of the momentum equations (full-system model) and a shallow ice approximation (SIA) model [*Hutter*, 1983]. This type of comparison has not been performed before. The full-system model includes gradients of all stress components in both spatial directions, while the SIA model ignores all horizontal stress gradients, leading to a greatly simplified description of glacier flow, where the flux at every point is related to the local surface slope and ice thickness. Furthermore, the full-system model uses a moving-mesh technique, allowing the position of the snout to be determined with high accuracy. The SIA model, on the other hand, uses a spatially fixed grid, a commonly used mesh method in glacier mechanics.

[4] The SIA has been used in most previous studies of the effects of mass balance changes on glaciers and ice sheets [e.g., *Oerlemans*, 2001], with the noticeable exception of the work of *Albrecht et al.* [2000] and *Vieli et al.* [2001]. The SIA forms the foundation of most current

[1]Now at Bristol Glaciology Centre, School of Geographical Sciences, University of Bristol, Bristol, UK.

[2]Now at British Antarctic Survey, Natural Environment Research Council, Cambridge, UK.

0148-0227/04/2003JF000027$09.00

mechanical models of ice sheets and ice caps [e.g., *Huybrechts*, 1992; *Hulbe and Payne*, 2001].

[5] *Raymond et al.* [1989] calculated changes in glacier length induced by climate change using several ice flow models of increasing complexity. They concluded that the initial reaction of glaciers to changing climate is a complex process requiring fairly sophisticated ice flow models. They suggested that the asymptotic approach to steady state can, on the other hand, be described using much simpler models.

[6] *Greuell* [1992] found that including longitudinal deviatoric stress gradients hardly affected the calculated response of Hintereisferner over timescales longer than ~100 years. Using SIA models for the calculation of shorter-term fluctuations was found to be problematic.

[7] *Pattyn* [2002] calculated the response of Haut Glacier d'Arolla to perturbations in thickness and mass balance using a full-system model and compared results with those of a SIA model. As he used an altitude-independent mass balance perturbation, the steady state geometry was the same for both models. The rate at which the glacier approached steady state differed, however; these differences were judged to be rather small for the particular mass balance forcing used, ~10%.

2. Model Description

[8] The gravity-driven transient evolution of an ice mass is calculated with a two-dimensional vertical plane flow model. The equations are written for a two-dimensional Cartesian geometry in an Eulerian reference frame with indices $i, j = 1, 2$, where the index 1 stands for the horizontal and 2 for the vertical component. The field equations to be solved describe the conservation of mass for incompressible materials,

$$v_{i,i} = 0,$$

and the conservation of angular and linear momentum,

$$\sigma_{ij} = \sigma_{ji} \quad \text{and} \quad \rho g_i + \sigma_{ij,j} = 0, \tag{1}$$

where v_i are the components of the velocity vector, σ_{ij} are the components of the Cauchy stress tensor, ρ is the material density, and g_i are the components of the gravity vector. The comma notation is employed, in which the indices following a comma imply a partial differentiation with respect to the corresponding spatial variable.

[9] A nonlinear power law [*Glen*, 1955; *Steinemann*, 1958] is used to describe the relationship between deviatoric stresses and strain rates:

$$\dot{\epsilon}_{ij} = A\,\tau^{n-1}\,\sigma_{ij}^{(d)}, \tag{2}$$

where $\dot{\epsilon}_{ij}$ are the strain rates and $\sigma_{ij}^{(d)}$ are the deviatoric stresses given by $\sigma_{ij}^{(d)} = \sigma_{ij} - (1/3)\delta_{ij}\sigma_{kk}$. The effective shear stress τ is defined by $\tau^2 = (1/2)\sigma_{ij}^{(d)}\sigma_{ij}^{(d)}$. In all model calculations the rate factor is assumed constant for the whole ice mass, and the flow law exponent n is taken to be 3.

[10] The free surface evolves according to the kinematic boundary condition

$$\frac{\partial z_s}{\partial t} + u_s \frac{\partial z_s}{\partial x} - w_s = \dot{b}(z), \tag{3}$$

where $z_s(x, t)$ describes the surface elevation, t is the time, u_s and w_s are the horizontal and vertical components of the flow velocity at the surface, respectively, and $\dot{b}(z)$ is the mass balance rate function. The mass balance rate function can be either a function of the glacier bed $z = z_b(x)$ or, more realistically, of the surface altitude $z = z_s(x, t)$ and therefore time-dependent. The velocities at the lower boundary are set to zero.

[11] Two different numerical models are used: (1) a full-system model, which solves all the terms of the above field equations, and (2) a shallow ice approximation (SIA) model [*Hutter*, 1983], which ignores all stress gradients other than the vertical gradient of shear stress. The SIA is that $\delta = d/l \ll 1$, where d is a typical ice thickness and l is a horizontal distance scale. It is common to refer to models solving the zeroth-order shallow ice equations simply as shallow ice approximation models.

[12] The implementation of the SIA model used here is based on finite differences on a fixed grid. The flux and slope are calculated by using centered differences at a staggered grid with a semi-implicit forward step in time. This is a standard approach often used in modeling of ice masses [*Hindmarsh and Payne*, 1996]. The terminus position is calculated as the first grid point where the ice thickness is zero and no subgrid tracking of terminus position is attempted. Discretization errors in terminus position were estimated by using different grid sizes and were found to be comparable to, or less than, the grid size.

[13] The full-system calculations were performed with the commercial finite element (FE) program MARC, adapted for use in glaciology by *Gudmundsson* [1999]. A four-node, isoparametric, quadrilateral Hermann element is used with a bilinear velocity interpolation. The code solves the full set of momentum equations and has been used extensively for flow modeling of alpine and of grounded tidewater glaciers [*Gudmundsson*, 1999; *Vieli et al.*, 2001]. The results of the numerical FE code have been verified in various ways, for example, by comparing calculated results with analytical solutions [*Gudmundsson*, 1997; *Aðalgeirsdóttir et al.*, 2000; *Raymond et al.*, 2003].

[14] The full-system model uses a moving grid, with the surface grid points moving every time step in both horizontal and vertical directions as needed in order to represent the new surface position as accurately as possible. The interior nodal points are then redistributed within the deforming body so as to minimize element distortion. This is done without affecting the connectivity of the finite element mesh or the number of nodal degrees of freedom. The structure of the system of equations does, hence, not change during the calculation. Since a direct solver is used, conserving the structure of the equations improves the numerical efficiency of the approach as no reassembling of the equation system is needed during a model run. It has been verified that the remeshing algorithm preserves volume accurately [*Leysinger and Gudmundsson*, 2000].

[15] The full-system model typically requires hours or days on a multipurpose parallel computer (HP-Superdome). With a SIA model, the same problem can be solved within minutes on a typical personal computer. Evidently, it is of considerable practical interest to be able to use the SIA whenever possible. It is, however, a nontrivial task to estimate the errors introduced by ignoring the horizontal stress terms. This can be done through a model intercomparison study. We find that although the velocities at the snout are strongly model-dependent, the differences in calculated rates of advance and retreat are small. This finding supports the macroscale approach to glacier mechanics advocated by *Oerlemans* [1989], *Jóhannesson et al.* [1989b], *Van der Veen* [1999], and *Harrison et al.* [2001].

3. Model Intercomparison Study

[16] The purpose of the model-model comparisons is to quantify the modeling errors introduced in calculating the retreat and advance of ice masses using a no-slip basal boundary condition when reduced numerical models such as the SIA models are used instead of the more complete full-system model. The SIA is an example of a long-wavelength approximation theory that assumes the aspect ratio (δ) to be small. How small δ must be for the errors to remain within certain bounds is a question to which it is difficult to give a general answer. If basal motion is small compared with the deformational velocity, the SIA is accurate to $O(\delta^2)$. The accuracy of the SIA is, however, expected to depend on other parameters besides δ, such as the relative contributions of internal ice deformation and of basal motion to the mean forward velocity [*Gudmundsson*, 2003].

[17] In some instances the aspect ratio becomes irrelevant for the accuracy of calculated quantities. For glaciers in steady state, for example, the horizontal flux at every location is given by the integral of the mass balance rate function over the catchment area upstream of that location. For a given mass balance distribution, any flow model which does not create or destroy mass will then produce accurate flux values and identical steady state lengths, irrespective of aspect ratios or rheological assumptions. If, however, the mass balance distribution depends on altitude, which is reasonable to expect, any model-dependent differences in calculated ice thicknesses will give rise to corresponding model-dependent differences in mass balance that will then further affect the ice thickness distribution. This mass balance altitude feedback effect can thus be expected to amplify any initial model-dependent differences in calculated glacier lengths and ice thicknesses. This illustrates the importance of doing model runs both with and without a mass balance altitude feedback. Furthermore, if a mass balance altitude feedback is included, the dependence of mass balance on altitude must be realistic.

[18] Calculations without a mass balance feedback are only of interest when done for glaciers not in steady state. If a glacier is far from steady state, the accuracy of the SIA can, for a given slip ratio (ratio of basal motion to deformational velocity), be expected to depend primarily on the aspect ratio. (How far a glacier is from steady state can be quantified through a comparison of the terms of the continuity equation relating specific mass balance rate $\dot{b}$, flux gradients $\partial_x q$, and rate of surface altitude change $\partial_t z$. If $\partial_t z \ll \dot{b}$ everywhere, the specific mass balance is closely balanced by flux gradients and the glacier can be considered to be close to a steady state.) Here we estimate model errors, not related to mass balance altitude feedback, by following the transient evolution of different blocks of ice characterized through an initial span-to-thickness ratio (modeling suite 1). To ensure that the ice blocks are never in steady state, the mass balance distribution is set to zero everywhere. Our primary interest is in quantifying differences in the rate of advance as a function of time. As the block of ice spreads out on a horizontal plane, its thickness decreases, and the aspect ratio becomes smaller. On the basis of this, one expects the rates of advance as calculated by a SIA and a full-system model to become progressively more similar with time. However, at any given time the SIA does not hold at the snout. Should the rate of advance be determined by local conditions at the snout only, model-dependent differences can therefore be expected to persist forever. As explained in detail in section 3.1, our findings are that apart from a relatively short initial period of time (on the order of a few tens of years ($\delta = 1$) to a few years ($\delta = 0.2$, 0.1)), both SIA and the full-system models do give rise to progressively similar rates of advance.

[19] The other situation considered here pertains to glaciers that are close to steady state and that have an altitude-dependent mass balance distribution (modeling suite 2). For an altitude-dependent mass balance distribution an identical thickness distribution is a sufficient condition for a SIA and a full-system model to produce identical steady state flux values. It is clear that the errors in ice thicknesses as calculated by the SIA may, in turn, be considered to be caused by aspect ratios that are too large. However, the aspect ratio alone does not control the size of the modeling errors. For a given aspect ratio, one can expect the differences in glacier lengths calculated by SIA and full-system models to increase with the strength of the mass balance altitude feedback. Furthermore, calculated thicknesses are also linearly related to the value of the rate factor (A). As its value is not accurately known, A effectively becomes a tunable model parameter that can be used to improve agreement between observed and calculated thickness distributions. Here we do not try to give a complete assessment of SIA modeling errors as a function of aspect ratio and the strength of the mass balance feedback effect, nor do we attempt to give a full answer to what extent model-dependent differences can be masked by varying the value of the rate factor. Rather, our approach here is to focus on situations that can be considered typical for alpine glaciers and to conduct case studies of small, medium, and large alpine glaciers using realistic mass balance distributions.

3.1. Modeling Suite 1: Geometry Evolution Experiments

[20] The lateral spread of the rectangular blocks bears a strong similarity to the self-similar solution of *Halfar* [1981]. As the Halfar problem is stable with respect to perturbations in surface shape that preserve volume, the profiles will settle down to the Halfar solution with time. A self-similar problem does, by its very nature, not have definable length scales. The height and the width evolve as $(h(x, t)/h_c(t))^{(1+1/n)} + (l(x, t)/s(t))^{(2+1/n)} = 1$, where $h_c(t)$ is

the center height and $s(t)$ is the span. For a given center height a timescale can be defined for the Halfar solution as the time since the ice cap may have evolved from an initial delta function of a given strength [*Nye*, 2000]. This timescale is clearly not of interest here. As the problem does not have definable length and timescales, rather than using dimensional variables, we normalize the results using the initial height and typical glacier surface velocities. Both spatial dimensions are normalized with the initial thickness of the block. The time is, somewhat arbitrarily, normalized with the ratio of thickness to the analytical solution of the deformational velocity for an infinite slab (analytical solution identical to shallow ice approximation) on a slope having an angle of 3°. For typical values of the rate factor A for temperate ice, one dimensionless time unit (T) corresponds to several decades. For rock glaciers, which are thinner and have much smaller surface velocities than typical alpine glaciers, the corresponding conversion factor is on the order of 1000 years.

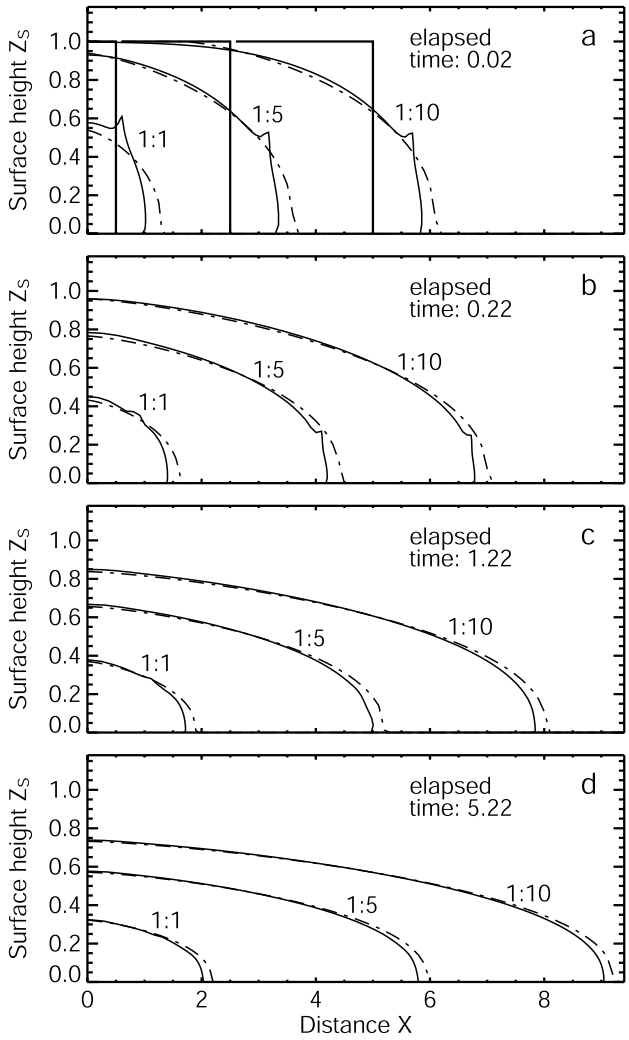

Figure 1. Surface evolution of three rectangles with different aspect ratios as calculated with a full-system model (solid lines) and a zeroth-order model (dash-dotted lines). (a) Initial surfaces at $t = 0$ and $t = 0.02$. (b–d) Surfaces at $t = 0.22$, 1.22, and 5.22, respectively. The times are nondimensional (see text). Note the different spatial scales.

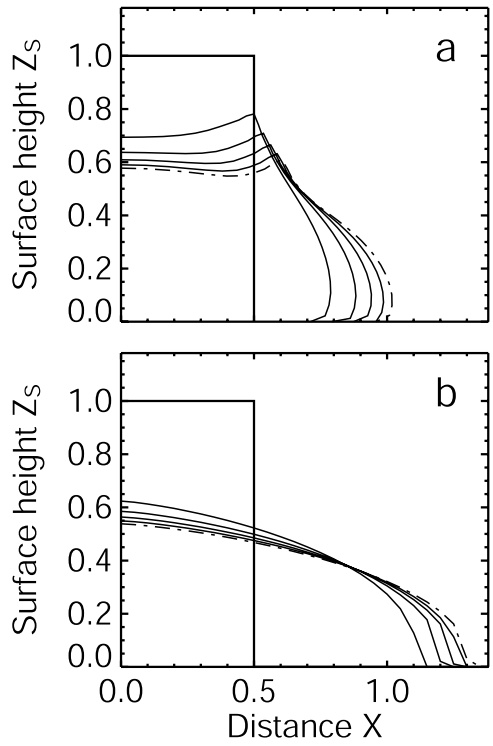

Figure 2. Surface evolution of a rectangle with an initial aspect ratio of 1 calculated with (a) a full-system model and (b) a zeroth-order model. The nondimensional time step between each plotted surface is 0.004 (see text). The thick solid lines and the dash-dotted lines correspond to the surface in Figure 1a.

[21] The transient evolution of rectangular blocks with initial heights h_0 and widths l_0 for three different initial aspect ratios $\delta = h_0/l_0 = 1$, 0.2, and 0.1 (Figure 1a) were calculated. Depending on the aspect ratios, the number of elements vary so that for $\delta = 1$, 20×20 elements are used, for $\delta = 0.2$, 10×50 elements are used, and for $\delta = 0.1$, 10×100 elements are used. Owing to the symmetry of the problem, only one half of the block was modeled.

3.1.1. Surface Evolution

[22] Figure 1 shows surface geometries at four different times as calculated with both the full-system model and the SIA model. For clarity, additional time steps are shown in Figure 2 for the block with the initial aspect ratio of $\delta = 1$.

[23] In Figure 2a, it can be seen how the full-system solution predicts the central part to initially sink down faster than the edges. With time, the amplitude of the surface depression becomes smaller, while the elevation minimum moves progressively toward what, at the start of the calculation, was the upper right-hand corner point. The surface depression eventually coalesces with the corner point and disappears. As is expected for a steep glacier margin, the horizontal velocity increases with depth over some distance, creating a zone of extrusion flow.

[24] A noticeable property of the full-system solution not shared by the SIA solution is that the corner point remains a visible feature for some time. The corner point can, for

example, still be seen at $t = 0.22$ (Figure 1b). At the corner point the boundary conditions require all stresses to be zero at the start of the calculation. For subsequent time steps the stresses acting on the corner are still low, and therefore the approximate shape of the corner point is preserved for some time (Figure 1). The SIA is known to lead to too short decay times at wavelengths comparable with and smaller than the mean ice thickness [*Gudmundsson*, 2003], and for that reason, the corner point disappears faster in the SIA model than it does in the full-system model.

[25] Figures 2a and 2b show the transient evolution of the $\delta = 1$ rectangle as calculated by the full-system and the SIA models, respectively. Note that the spatial scales are the same in both figures. A comparison of Figures 2a and 2b illustrates some of the key model-dependent differences. The surface shapes and velocities are qualitatively different, with the full-system surface being concave, whereas the SIA gives a convex surface shape. In the SIA, flow velocities are always directed in the direction of the steepest slopes. Surface troughs and hollows can therefore only exist for a limited amount of time as they must eventually get filled up with ice. For this reason, one generally expects surfaces calculated using the SIA to be convex. The SIA cannot produce an increase in forward velocities with depth and therefore no extrusion flow is seen in Figure 2b.

3.1.2. Rate of Advance

[26] At the start of the calculation the slope at the upper-right corner point is discontinuous. The velocities calculated with the SIA at that point depend, however, on the local ice thickness and surface slope. In the particular numerical implementation of the SIA used here (which is a standard finite difference approach often used in modeling of ice masses) the flux and slope are calculated by using centered differences at a staggered grid with a semi-implicit forward step in time. For a given spatial discretization, with flux and slope calculated at a staggered grid, a finite value is obtained for the surface slope at the corner point, and consequently, a finite velocity is obtained at that point as well. However, this velocity depends on the particular grid spacing used, approaching infinity as the grid spacing shrinks to zero. At the first time step of the SIA model, this corner is the only point of the surface with a nonzero velocity. During subsequent steps the velocities become nonzero to the left and the right of the corner point at a rate that is dependent on the size of the time step and the exact discretization scheme used. Clearly, the velocities around the corner point are not only wrong by an arbitrary amount at the start of the calculation but also do not fulfill grid size independence, which is a basic requirement for a correct numerical solution. One might therefore expect that not only the velocities at the snout, as calculated using the SIA, but also the rate of advance of the snout will be incorrect.

[27] By comparing the position of the snout obtained by both models in Figure 1 and by comparing the slopes of the curves in Figure 3, it becomes clear that this is, however, not the case. Figure 1 shows that early in the calculation, the front positions calculated with the SIA model are farther to the right than those of the full-system model. As time proceeds, these differences, however, become progressively smaller. In Figure 1d, these differences are 9% (3.5 times the SIA grid sizes) for $\delta = 1$, 3.5% (2.1 times SIA grid sizes) for $\delta = 0.2$, and 2.5% (2.3 times the SIA grid sizes) for $\delta = 0.1$.

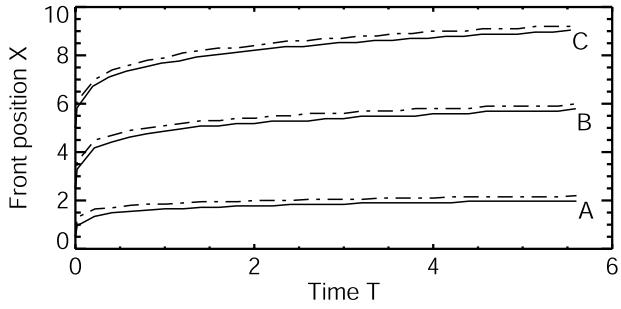

Figure 3. Front position as a function of time for different initial aspect ratios (A = 1, B = 0.2, C = 0.1) and for both the full-system model (solid lines) and the SIA model (dotted lines).

[28] As the rectangles spread out, their aspect ratios go asymptotically to zero and with them the errors of the SIA model. Both models converge toward the same geometry, which can be seen as a consequence of the stability of the Halfar solution with respect to perturbations in the surface profile that conserve volume [e.g., *Halfar*, 1981; *Hindmarsh*, 1990; *Nye*, 2000]. Comparing Halfar's analytical solution for the surface profile with the SIA surface profile shows that the differences drop almost immediately below 1% (e.g., at $T = 0.004$ for $\delta = 1$) over most of the model domain. Differences of more than a few tenths percent are only observed at the very margin, and the differences become smaller with time. For the full-system model, deviations in surface profile from the Halfar solution are, at every time step, larger than those of the SIA model. This is to be expected as the Halfar solution is derived by assuming the flux to be a local function of thickness and slope. For T larger than $\sim$3.2 and $\delta = 1$ the difference in the central surface height ($x = 0$) between the two models is <2%. For $\delta = 0.2$ and $\delta = 0.1$ thedifference becomes <2% for $T > 1.4$ and 0.4, respectively (Figure 1).

[29] Figure 3 shows the position of the snout as a function of time. The slopes of the curves give rates of advance. There is some initial offset between curves calculated with the SIA model and the full-system model. This offset is caused by differences in calculated rates of advance at the very beginning of each model run. Although not easy to see in Figure 3, the curves converge with time.

[30] The horizontal velocity component along the surface at different times is shown in Figure 4 for the three different values of δ and for both the full-system and the SIA models. Near the front, surface velocities calculated with the two numerical models are significantly different at all times. This is to be expected. At the snout, surface slopes tend to infinity and with it the velocities as calculated using the SIA. Again, the reason why the SIA model does not produce infinite velocity is because of the finite distance between the nodes of the numerical grid. Hence, although the overall surface shapes and the rate of advance of the front position are insensitive to the different sets of assumptions on which the two numerical models are based, the surface velocities at the front remain different. For the block with $\delta = 1$, Figure 4 shows that the two velocity profiles

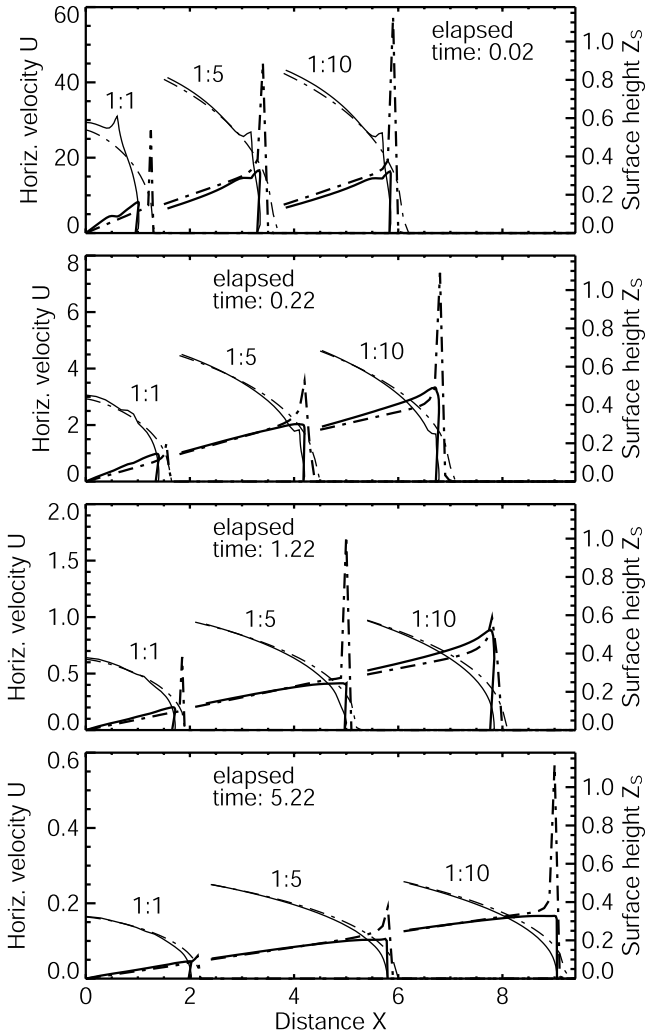

Figure 4. Surface velocities (thick lines) and surface profile (thin lines, note different spatial scales) as a function of distance at different times, calculated with a full-system model (solid lines) and the SIA model (dash-dotted lines) for three different initial aspect ratios. The center of each model is at $x = 0$, but for clarity, not all profiles are shown in their entirety.

(SIA and full-system) are most similar in the central area. Apart from the region next to the snout, both sets of velocities become progressively more similar with time for all initial aspect ratios (Figure 4).

3.2. Modeling Suite 2: Advance and Retreat of No-Slip Alpine-Type Glaciers

[31] The numerical experiments with rectangular blocks discussed in section 3.1 showed that for all initial aspect ratios the surface geometry, the front position, and the advance velocity became progressively more similar as both models were integrated forward in time. The question now arises as to whether including mass balance altitude feedback and using more realistic glacier geometries changes the situation significantly.

[32] As a first step, model runs are performed using a x-dependent mass balance distribution. Thus, there is no altitude mass balance feedback and the modeled steady state front positions must be equal for both models. This position can be determined analytically, allowing the accuracy of the numerical models to be estimated.

[33] In a second, and more interesting, step the evolution of three differently sized alpine glaciers are calculated with a realistic mass balance altitude function. The mass balance rate function is of the form

$$\dot{b}(z) = \begin{cases} a_{\mathrm{acc}}(z_s - \mathrm{ELA}) & \text{when} \quad z_s > \mathrm{ELA} \\ a_{\mathrm{abl}}(z_s - \mathrm{ELA}) & \text{when} \quad z_s \leq \mathrm{ELA} \end{cases}, \tag{4}$$

where ELA is the equilibrium line altitude and a_{abl} and a_{acc} are the mass balance gradients below and above the equilibrium line, respectively. The values for the mass balance gradients are set to $a_{\mathrm{acc}} = 2.8 \times 10^{-3}$ a^{-1} and $a_{\mathrm{abl}} = 6.7 \times 10^{-3}$ a^{-1}. These particular values are derived from mass balance data from Griesgletscher for the observation period of 1994–1995 [*Herren and Hoelzle*, 1991] but are also rather typical of other alpine glaciers and other time periods [e.g., *Oerlemans*, 2001, pp. 41–44]. The ELA is arbitrarily set at 2801 m above sea level (asl). The equilibrium line altitude is then perturbed, and the transient evolution of the glaciers is followed in detail until a new steady state is established. The transient response to spatially confined mass balance perturbations acting over a limited period of time is also investigated.

3.2.1. Model Setting

[34] The three prototype glaciers correspond in terms of lengths l, mean slopes, and absolute heights to a small (1 km $\leq l <$ 5 km), a medium-sized (5 km $\leq l <$ 10 km), and a large ($l \geq$ 10 km) valley glacier, respectively, following the glacier length classification of *Herren et al.* [1999] for Swiss glaciers (Figure 5). Grosser Aletschgletscher has been chosen to represent a large glacier with a maximum altitude of 4140 m asl, a length of 24.7 km, and a mean slope of 6.1°. Griesgletscher has been chosen to represent a medium-sized glacier with a maximum altitude of 3360 m asl, a length of 6.2 km, and a mean slope of 9.0°. Finally, Ghiacciaio del Basodino is used to represent a small glacier with a maximum altitude of 3220 m asl, a length of 1.6 km, and a mean slope of 26.0° [*Müller et al.*, 1976].

[35] The three chosen glaciers are located in three different valleys in the central Swiss Alps. Despite some expected differences in local climate, the different glacier lengths are presumably mainly related to variations in bed slope [*Schmeits and Oerlemans*, 1997; *Oerlemans*, 2001]. Thus we assume that all three model glaciers are exposed to the same climatic conditions, and we use the same mass balance rate function for all three glaciers. The bed topography is parameterized using two differently inclined planes. The steep upper plane (45°) is of short horizontal distance (1/20 of the maximum length) and corresponds to a headwall which frames the upper bound of the glaciers. The lower plane is inclined by 4.5° for the large glacier, by 5.5° for the medium-sized glacier, and by 23.5° for the small glacier (Figure 5). This leads to an average slope for each glacier corresponding closely to that of the prototype.

[36] For each glacier the model calculation starts from a steady state situation calculated using an initial ELA of 2801 m asl (hereinafter referred to as initial steady state).

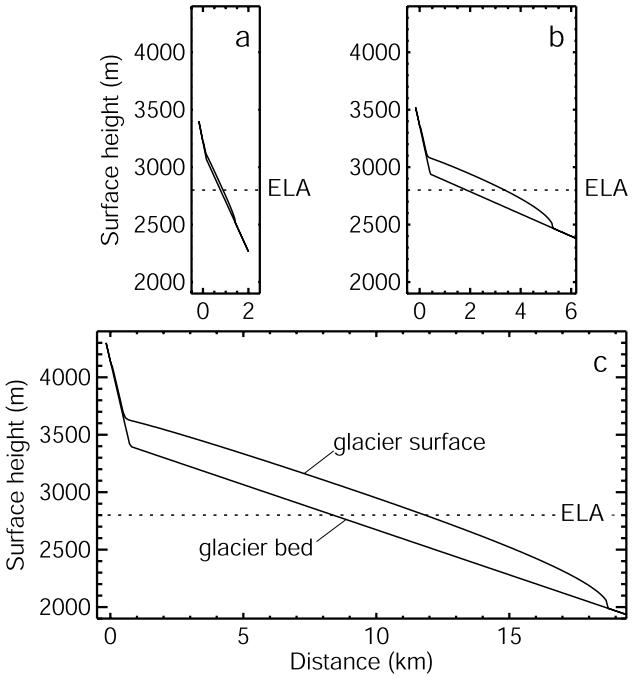

Figure 5. Initial SIA steady state geometries of the three "prototype" alpine glaciers. The ELA was set at 2801 m above sea level: (a) the small, (b) the medium-sized, and (c) the large glacier are shown using identical scalings.

Advance and retreat are caused by shifting the ELA by ±100 m. In all experiments with the full-system model the number of elements is kept constant (10 × 160). The sizes of the elements vary logarithmically, with the smallest elements close to the margins.

3.2.2. Reaction Ignoring Mass Balance Altitude Feedback

[37] In the absence of a mass balance altitude feedback the relationship between the change in length Δl and a given perturbation in the mass balance rate $\Delta \dot{b}$ is independent of rheology and dynamics of flow. For example, for a linear variation in mass balance rate $\dot{b}$ (x) with horizontal distance x the relation is $\Delta \dot{b} l_o + \dot{b}(l_o)\, \Delta l = 0$, where $\Delta \dot{b}$ is the uniform shift in mass balance rate, l_o is the original position of the terminus, and $\dot{b}(l_o)$ is the nonperturbed mass balance rate at the original terminus position [*Nye*, 1960]. There is no such relationship between the perturbation in mass balance rate and the resulting perturbation in volume. The volume perturbation can only be calculated by making some assumptions about glacier flow, rheology, and bedrock geometry.

[38] For both models, calculated front positions agreed with the analytical solution (3287 m). Errors for the SIA model were within the grid resolution of 10 m. As an example, for the medium-sized glacier, differences between calculated and correct length were 7 and 0.1 m for the SIA and the full-system models, respectively.

[39] Figure 6 shows the length and volume changes for the medium-sized glacier for both an advance and a retreat. The initial steady state volume of the full-system model was ~4.1% larger than the volume of the SIA model. The cumulative volume change was, however, essentially identical. There is a slight asymmetry in length and volume change with respect to retreat and advance (Figure 6) which is related to the mass balance rate distribution not being a strictly linear function of distance. Here the mass balance distribution is described with two linear functions linked at ELA (equation (4)). If the mass balance rate distribution were a linear function of distance, the perturbation in length would be twice the horizontal shift in ELA and symmetric with respect to retreat and advance.

3.2.3. Reaction Including Altitude Mass Balance Feedback

[40] Now an altitude-dependent mass balance function is used for both numerical models. First, the initial steady states for an ELA at 2801 m asl were calculated using both models for all three glaciers. Starting from these initial steady states, the advances and retreats to new steady states were then determined.

3.2.3.1. Initial Steady State

[41] The initial steady state geometries calculated by the full-system model are generally thicker than those calculated with the SIA model (Table 1). The difference between the initial full-system and the initial SIA steady state surface at the SIA grid points is shown in Figure 7. The largest differences in surface shapes between the two models are found where the errors of the SIA can be expected to be largest, which is along the upper steeper slope and at the front. These differences in the surface are largest for the small glacier and smallest for the large glacier. As a fraction of their corresponding thicknesses, these model-dependent differences can be considered to be insignificant for both the medium-sized and the large-sized glaciers (3.8% and 1.6%, respectively) but significant for the small glacier (17.0%). These model-dependent differences in initial steady state

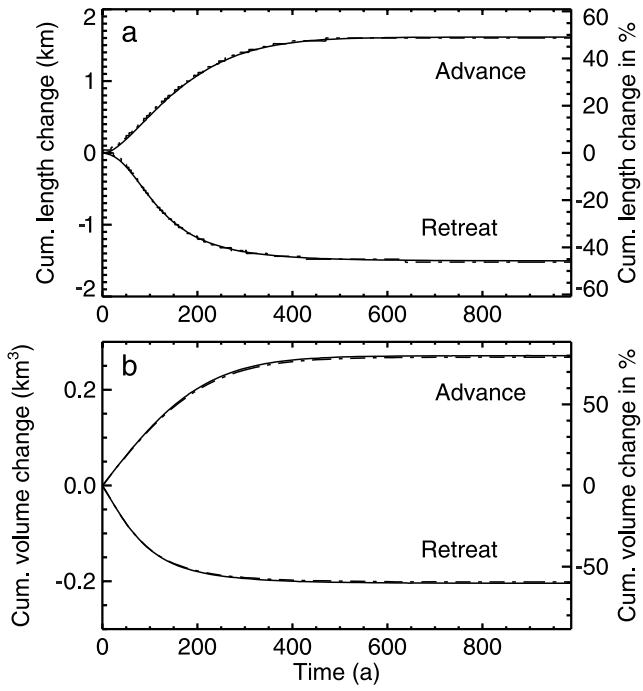

Figure 6. (a) Cumulative length and (b) volume changes of the medium-sized glacier as functions of time and as calculated using a full-system (solid lines) and a SIA (dash-dotted lines) model with no mass balance altitude feedback.

Table 1. Differences in Length and Volume for the SIA Results Compared With the Full-System Results With an Altitude-Dependent Mass Balance

	Length Difference			
Glacier Size	Percent	SIA Grid Sizes	Grid Size, m	Volume Difference, %
Small	−2.6	−3.7	10	−18.5
Medium	−1.2	−1.6	40	−4.1
Large	−0.6	−1.5	80	−1.6

volume and length are caused by an overall increase in ice thickness in the full-system model needed to overcome horizontal stresses. In the SIA model the flux depends only on the local surface slope and the local thickness, whereas in the full-system model the overall glacier geometry can, to some extent, affect the local flux through transmission of horizontal stresses. In the vicinity of the snout, horizontal stresses act to hinder the motion. As a consequence, ice thicknesses become larger as compared with those of the SIA model. Because of the mass balance altitude feedback, the increased overall thickness leads to an increased total glacier length. Small additional differences are due to the different meshing techniques of the two models. The full-system model uses an adaptive grid that moves with the surface. The front position is therefore not bound to a set of spatially fixed nodal points, as in the SIA model. The errors in terminus positions of the SIA model are comparable to the grid spacing. Those grid size effects on calculated front positions could be estimated rather easily by using a number of meshes having different grid sizes. Grid spacing was thus kept small enough for the purpose of the model intercomparison. No subgrid tracking of the terminus [e.g., *Lam and Dowdeswell*, 1996] was attempted, but doing so would not have affected our conclusions nor have had any significant impact on computing time.

3.2.3.2. Advance and Retreat

[42] By shifting the ELA accordingly, the glaciers were forced to either advance or retreat. In contrast to the altitude feedback-independent case discussed in section 3.2.2, we can now, in principle, expect some model-dependent differences in cumulative length and volume changes. The calculated cumulative length and volume changes are shown in Figures 8 and 9 for both models. Differences in calculated lengths larger than one grid size of the SIA model are only obtained for the small glacier (2 grid cells, 1.2% of the glacier length). Figure 9 shows the difference in cumulative volume change. Again, only for the small glacier can significant volume differences be seen (∼17.5% of the final volume). Where differences are found, the SIA model produces a larger advance and a shorter retreat than the full-system model (Figure 8a).

[43] As a fraction of the original steady state length, the cumulative length change is largest for the medium-sized glacier and smallest for the large glacier. This is also reflected in the fractional volume changes (Figures 8 and 9, right vertical axis).

[44] The relative length and volume changes for the advance and the retreat from the initial steady states are shown in Table 2. For an advance the relative volume change is slightly larger than for a retreat. This difference between volume gain and volume loss for the same absolute shift in ELA is model-dependent and turns out to be larger for the SIA model than for the full-system model. In numbers, these differences are 18%, 13%, and 5% for the small, medium, and the large glacier, respectively, when calculated with the SIA model. Using the full-system model, the corresponding numbers are 10%, 13%, and 4%.

[45] Following the evolution of the front position and the volume with time (Figures 8 and 9), we see that for both models, ignoring the initial phase, the rate of advance and retreat and the rate of volume change of the medium-sized and large-sized glaciers are identical (Figures 10b and 10c). For the small glacier, however, a significant model-dependent difference in volume change rate is observed over most of the adjustment period (Figure 10a). For this glacier the inclusion of horizontal stresses in the force balance leads to elevation changes that, when combined with the mass balance altitude rate function, causes noticeable differences in rates of advance and retreat (see Figures 8a and 9a). For all three prototypes the volume decrease rates are higher than the volume increase rates.

[46] The time span needed for a glacier to find a new steady state after a change in mass balance (Figures 8 and 9) is quantified by the (asymptotic) response time, which can be defined as the time constant in an exponential asymptotic approach to a final steady state after a sudden change in climate to a new constant climate [*Jóhannesson*, 1997]. The volume e folding time is the time it takes for the glacier volume perturbation ΔV to reach e^{-1} (retreat) or $1 - e^{-1}$ (advance) of its final steady state value, i.e., $\Delta V = \Delta V_\infty(1 - e^{-t/\tau_V})$, where ΔV_∞ is the volume perturbation in the limit $t \rightarrow \infty$. In general, the e folding time and the asymptotic

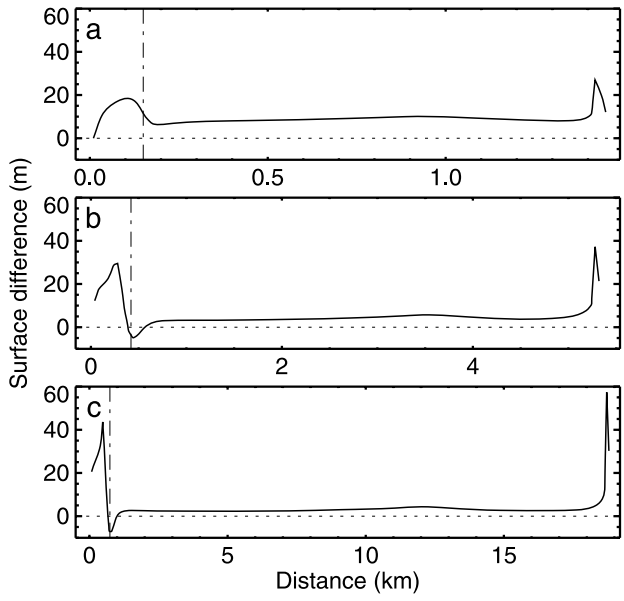

Figure 7. Difference in initial steady state geometries calculated by the two models shown for (a) the small glacier, (b) the medium-sized glacier, and (c) the large glacier. For the full-system model the surface has been calculated at the grid points of the SIA model. A positive difference corresponds to a greater ice thickness for the full-system model. The location of the break in the bed slope is shown as a dash-dotted line.

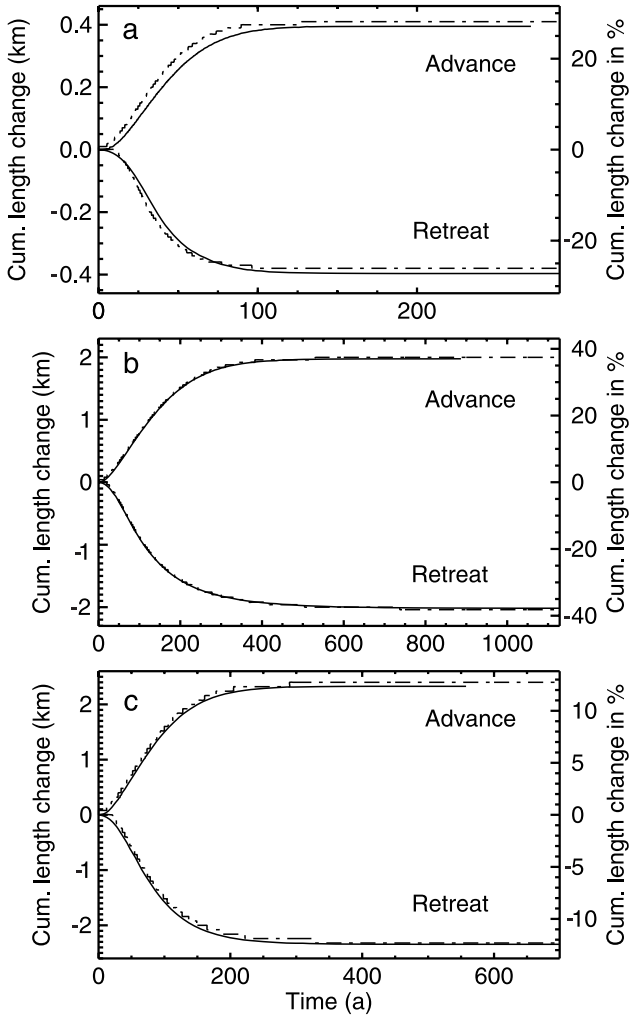

Figure 8. Cumulative length changes of all three prototype glaciers as functions of time calculated using a full-system (solid lines) and a SIA (dash-dotted lines) model with mass balance altitude feedback: (a) small, (b) medium-sized, and (c) large glacier.

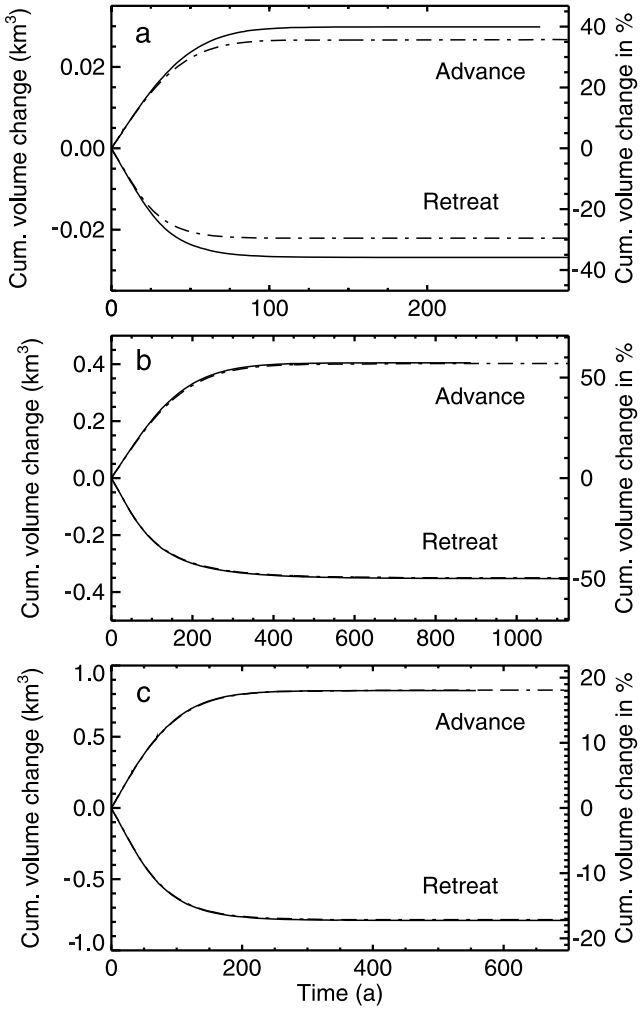

Figure 9. Cumulative volume changes of all three prototype glaciers as functions of time calculated using a full-system (solid lines) and a SIA (dash-dotted lines) model with mass balance altitude feedback: (a) small, (b) medium-sized, and (c) large glacier.

response time will not be identical. We estimated both the *e* folding time and the asymptotic response time but found the *e* folding time to be easier to determine as the change in volume and length as a function of time was often far from being exponential. In the following, if not otherwise stated, the "response" times are *e* folding times.

[47] Because of mass conservation, the glacier volume must always immediately start to change following an abrupt shift in mean cumulative mass balance. The glacier length, on the other hand, may only start to react to mass balance changes after an initial time lag (the length time lag). In all model runs the length time lag was always much shorter than the length response time, and no attempt was made to determine it accurately or to subtract the length time lag from the *e* folding time.

[48] In Table 3 the *e* folding times of each glacier are listed for an advance and a retreat and for both the full-system and the SIA models. Table 3 shows that the volume response time (τ_{Vn}) is shorter than the length response time (τ_{Ln}) for all three glaciers, in agreement with the findings of *Schmeits and Oerlemans* [1997] for their one-dimensional SIA flow line model of Unterer Grindelwaldgletscher. For a retreat, these differences in volume and length response times are even bigger.

[49] Ignoring mass balance altitude feedback, *Jóhannesson et al.* [1989a, 1989b] and *Jóhannesson* [1997] give a

Table 2. Length and Volume Changes for Both the Full-System (FS) and the SIA Model After an Advance and a Retreat Relative to the Initial SIA Steady State Position L_{SIA} and Volume V_{SIA}, Respectively

		$\Delta L/L_{SIA}$		$\Delta V/V_{SIA}$	
Glacier Size	Model	Advance	Retreat	Advance	Retreat
Small	FS	0.278	−0.279	0.490	−0.440
	SIA	0.289	−0.268	0.439	−0.362
Medium	FS	0.374	−0.382	0.598	−0.520
	SIA	0.379	−0.386	0.594	−0.516
Large	FS	0.124	−0.125	0.183	−0.175
	SIA	0.128	−0.124	0.184	−0.174

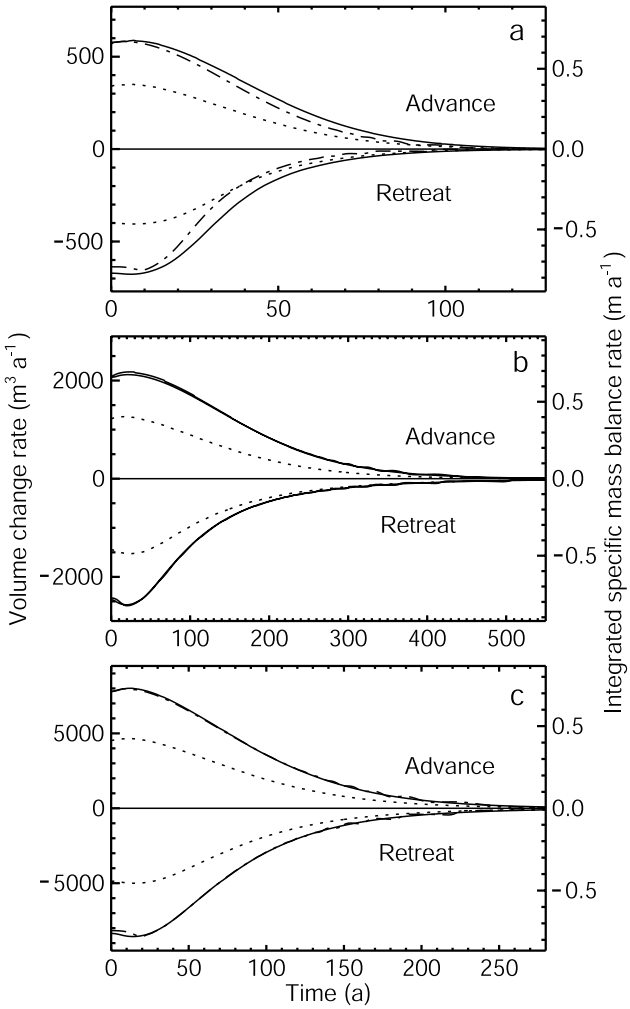

Figure 10. Volume change rate for the advance and the retreat as a function of time for (a) the small glacier, (b) the medium-sized glacier, and (c) the large glacier, calculated with both the full-system model (solid lines) and the SIA model (dash-dotted lines). The right vertical axis gives the integrated specific mass balance rate (dotted lines).

theoretical estimate of the volume response time τ_V, which is given by

$$\tau_{Vj} = -h_{\max}/\dot{b}_t, \tag{5}$$

where $h_{\max}$ represents the maximum thickness of the glacier and $\dot{b}_t$ represents the average mass balance for the region exposed by a retreating glacier or covered by an advancing glacier. Both the numerical and the theoretical Jóhannesson volume response times are shortest for the small-sized glacier and longest for the medium-sized glacier (Tables 4 and 5).

[50] The (numerical) volume response times determined from the results of the numerical models are, however, significantly different from those (theoretical) volume response times predicted by equation (5). This is not surprising. The derivation of equation (5) ignores the mass balance altitude feedback. Including mass balance feedback will always lead to increased reaction times as any adjustment in glacier geometry must lead to new, additional changes in mass balance that require a further adjustment in glacier shape.

[51] *Harrison et al.* [2001] defined a volume timescale (τ_{Vh}), which explicitly includes the effect of surface elevation on mass balance rate to characterize the glacier response to climate. They find that

$$\tau_{V_h} \equiv \frac{1}{-\frac{\dot{b}_e}{H} + \dot{G}_e}, \tag{6}$$

where $\dot{G}_e$ is the weighted average of the specific balance rate gradient, $\dot{b}_e$ is the specific balance on the bedrock surface and averaged over the entire exposed/covered region (defined by *Elsberg et al.* [2001, equations (9) and (10)]), and $H = \Delta V/\Delta A$ is the thickness scale.

[52] The timescale τ_{Vh} has the same interpretation as τ_{Vj} but with the significant difference that τ_{Vh} accounts explicitly for the effect on balance rate of the changing surface elevation of the glacier via the $\dot{G}_e$ term [*Harrison et al.*, 2001]. The dependence of the mass balance rate on surface

Table 3. Numerical Response Times in Years for Volume τ_{Vn} and Length τ_{Ln} Calculated for an Advance and a Retreat With Both the Full-System (FS) and the SIA Model for All Three Prototype Glaciers

	Small		Medium		Large	
	FS	SIA	FS	SIA	FS	SIA
			τ_{Vn}			
Advance	36	33	133	136	75	76
Retreat	27	23	105	105	66	66
			τ_{Ln}			
Advance	49	42	158	158	98	94
Retreat	43	39	145	150	93	98

Table 4. Numerical and Theoretical Response Times for Volume (τ_{Vn}, τ_{Vj}, and τ_{Vh}) Calculated for an Advance With the Full-System Model for All Three Prototype Glaciers[a]

	Small	Medium	Large
τ_{Vn}	36	133	75
τ_{Vj}			
$H = h_{\max}$	**32**	**72**	**52**
$H = \Delta V/\Delta A$	41	93	66
τ_{Vh}			
$H = h_{\max}$	40	125	76
$H = \Delta V/\Delta A$	**54**	**209**	**110**

[a]Times are in years. By respective author (*Jóhannesson et al.* [1989a], *Jóhannesson et al.* [1997], and *Harrison et al.* [2001]), suggested theoretical response times are in boldface.

Table 5. Numerical and Theoretical Response Times for Volume (τ_{Vn}, τ_{Vj}, and τ_{Vh}) Calculated for a Retreat With the Full-System Model for All Three Prototype Glaciers[a]

	Small	Medium	Large
τ_{Vn}	27	105	66
τ_{Vj}			
$H = h_{\max}$	**29**	**69**	**51**
$H = \Delta V/\Delta A$	33	77	62
τ_{Vh}			
$H = h_{\max}$	36	122	75
$H = \Delta V/\Delta A$	**43**	**148**	**99**

[a]Times are in years. By respective author (*Jóhannesson et al.* [1989a], *Jóhannesson et al.* [1997], and *Harrison et al.* [2001]), suggested theoretical response times are in boldface.

elevation has a major effect on the response and leads to longer timescales than those calculated by *Jóhannesson et al.* [1989a, 1989b]. *Oerlemans* [2001] has suggested a response time for glacier length including mass balance feedback which bears strong similarities to the Harrison timescale [*Oerlemans*, 2001, equation (9.15)] and finds that including mass balance feedback may easily double or triple the response time.

[53] This effect of surface elevation on the response time can be shown by calculating both Harrison's and Jóhannesson's theoretical response times with the same averaged specific mass balance $\dot{b}_e = -\dot{b}_t$ and the same thickness scale H. To investigate the significance of the chosen thickness scale, we calculate both timescales with $H = \Delta V/\Delta A$ as chosen by *Harrison et al.* [2001] and $H = h_{max}$ as chosen by *Jóhannesson* [1997]. In our case, $H = \Delta V/\Delta A$ is 10–30% larger than $H = h_{max}$. The theoretical response times, calculated for both an advance and a retreat from the initial steady state, obtained from the two numerical models for all three glaciers are shown in Tables 4 and 5, along with the numerical response times. Comparing the numerical response times with the ones from *Jóhannesson* [1997] calculated with $H = h_{max}$ and the ones from *Harrison et al.* [2001], calculated with $H = \Delta V/\Delta A$, we find that the *Jóhannesson* [1997] response times are generally smaller and that the *Harrison et al.* [2001] response times are generally larger than the numerical response times. Closer investigation of the response times shows that the advance and the retreat, except for the small glacier, are best described by *Harrison et al.* [2001] response time τ_{Vh} with the thickness scale $H = h_{max}$. The small glacier is best described by *Jóhannesson*'s [1997] response time τ_{Vj} with $H = h_{max}$. The *Harrison et al.* [2001] response times calculated with $H = \Delta V/\Delta A$ tend to be larger than the numerical volume response times but show good agreement with the length response times for the small and the large glacier (Table 3). Note that a change in thickness scale has a larger effect on τ_{Vh} than on τ_{Vj}. We find that ignoring the altitude dependency of the mass balance (using an x-dependent mass balance function) results in response times similar to, albeit somewhat shorter than, the theoretical estimate given by equation (5).

[54] By comparing the numerical response times (Tables 3, 4, and 5) for the advance and the retreat, it can be seen that, with one exception, the response times are shorter for the retreat than for the advance. This is in agreement with the results discussed above and shown in Table 2 and Figure 10. The theoretical response times calculated both with $H = h_{max}$ show only negligible differences between a retreat and an advance.

[55] From Table 3 we see that both the SIA and the full-system models give similar volume response times τ_{Vn}, with the exception of the small glacier, where significant model-dependent differences are observed. The small glacier shows that numerical response times τ_{Vn} calculated from the SIA model are 8% smaller for the advance and 15% smaller for the retreat than those obtained from the full-system model. For the small glacier the theoretical response times are compared to the numerical response times obtained from the full-system model. The theoretical *Jóhannesson* [1997] response time τ_{Vj} calculated with $H = h_{max}$ (Tables 4 and 5) for the small glacier results in response times which are 10% smaller for the advance and 8% larger for the retreat than the numerical response times (14% and 22% larger when calculated with $H = \Delta V/\Delta A$). The theoretical *Harrison et al.* [2001] response time τ_{Vh} with $H = \Delta V/\Delta A$ results in 52% (advance) and 56% (retreat) larger response times than those obtained by the numerical method (12% and 33% smaller when calculated with $H = h_{max}$). This example shows that the response times depend not only on the chosen formulation of timescale but also on the thickness scale H. For the two larger glaciers the response time τ_{Vn} is insensitive to differences between the full-system and the SIA model. This supports the result of *Greuell* [1992] that the effect of longitudinal stress gradients on the response times is small.

3.2.4. Short-Term Mass Balance Perturbation

[56] In the previous set of experiments we investigated model-dependent differences in the calculated response of alpine glaciers when the ELA is abruptly shifted. Those step changes in mass balance were large. Small-scale fluctuations are superimposed on the large-scale fluctuations of the climate signal. The question arises, How do the two models compare when the evolution of a short-term mass balance perturbation is calculated? To investigate this, we now consider perturbations in the mass balance distribution that are confined to a local area and are of limited temporal duration.

[57] In a first experiment a perturbation is added to the standard altitude-dependent mass balance function for the first 5 years. An example of a spatially localized mass balance perturbation $\Delta\dot{b}$ is a Gaussian-shaped bulge:

$$\Delta\dot{b} = B\exp\left[-\frac{1}{2}\left(\frac{x - x_o}{\sigma}\right)^2\right]. \quad (7)$$

The mean position of the perturbation peak (x_o) is assumed to be in the middle of the accumulation area. B is the amplitude and σ is the width of the perturbation. As before, the model runs start from a steady state configuration. At the beginning of the model run the mass balance perturbation $\Delta\dot{b}$ is added to the altitude-dependent mass balance. The calculations were carried out for the small and the large glacier using $B = 4$ m a^{-1} and $\sigma = 5\%$ of the initial steady state glacier length. Figure 11 shows the resulting evolution of volumes and front positions.

[58] For the small glacier the maximum in volume and length is reached 6.5 and 9 years earlier in the SIA model than in the full-system model, respectively (Figure 11). This result may be due to the fact that at spatial scales that are short compared with the mean ice thickness, harmonic surface undulations decay much faster in a SIA model than in a full-system model [*Gudmundsson*, 2003].

[59] For the large glacier, both models showed almost identical temporal volume and length changes (Figure 11c and 11d). Using a smaller amplitude of 2 m a^{-1} and a larger half width of 10% gave similar results.

[60] In a second experiment in which the ELA was lowered temporarily by 250 m for 5 years, both models produced essentially identical transient changes in volumes and lengths for both glaciers. This finding demonstrates nicely that for spatially uniform perturbations in mass balance forcing the SIA appears sufficiently accurate to calculate the effects of short-term climatic variations on alpine glaciers.

[61] Recapitulating, we find that for localized surface disturbances the overall adjustment is slower when calcu-

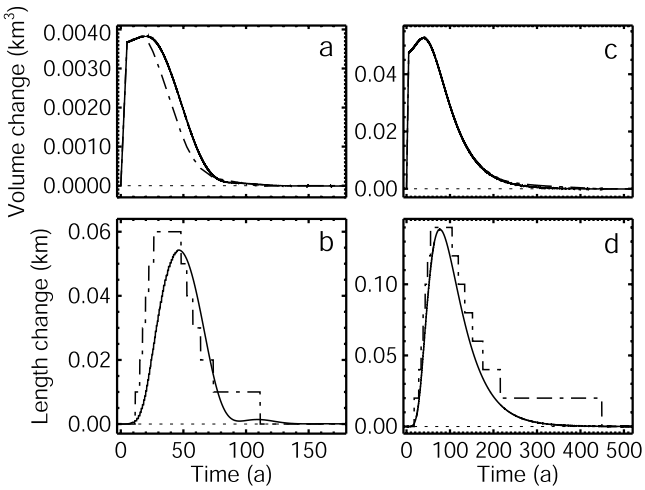

Figure 11. (a and c) Volume and (b and d) length changes as a function of time after a small mass balance perturbation has been added to the accumulation area during the first 5 years of model runtime. Figures 11a and 11b show results for the small glacier, and Figures 11c and 11d show results for the large glacier. The changes calculated with the full-system model are shown with solid lines, and the ones with the SIA model are shown with dash-dotted lines.

lated by the full-system model than by the SIA model. On the other hand, for glacier-wide changes in mass balance such as those resulting from a uniform shift in ELA the temporal behavior is essentially model-independent. Both of these findings can be understood in terms of the differences between the relaxation spectrum of the SIA model and the full-system model. Localized surface disturbances decay faster in a SIA model than in a full-system model. This is to be expected. By linearizing both models, it can be shown [*Gudmundsson*, 2003] that these models give rise to decay times that differ by several orders of magnitude at short spatial scales, with the SIA model giving estimates for the decay timescale that are too short.

4. Discussion

[62] The two models differ in their treatment of the mechanics of glacier flow. The SIA leads to considerable simplifications of the underlying set of equations, and the picture of glacier mechanics that emerges from that approximation is simple. The full-system model, on the other hand, gives a full description of the mechanics of glacier flow for the particular set of assumptions about basal conditions and rheological properties of ice used here.

[63] The first suite of experiments with the rectangles showed that despite the velocities at the snout being very different for the two models (Figure 4), and despite the SIA model velocities not being independent of grid size (tending toward infinity as the grid size goes to zero), the front position given by the SIA agrees well with the position calculated with a full-system model (Figure 1). Furthermore, the model-model comparison shows that the advance rates of the snout, calculated with the two numerical models, are almost identical (Figure 3). The second modeling suite demonstrates that this observed model independence of the advance and retreat rates is also valid for most realistic alpine glacier geometries.

[64] This model independence of the snout position and advance and retreat rates can be understood in terms of mass continuity. Although at any particular point in time the rate of advance of the snout may depend on the details of the velocity profile and the shape of the surface at the snout, the mean advance of the snout over extended time periods must ultimately be related to the vertically integrated mass flux some distance behind the front. Particularly when ice masses are close to steady state, one would therefore expect length changes to be related to the integrated imbalance in mass fluxes along the whole surface of the glacier and not to depend on the details of the flow field at the snout. As shown in this paper, for both models the calculated rates of advance and retreat are almost identical, although their description of flow dynamics close to the snout is fundamentally different. With respect to the reaction of the glaciers to shifts in ELA, the choice of the model is important only for the small glacier and even then only when an altitude-dependent mass balance function is used.

[65] In this study, any possible basal motion has been ignored, and we can only speculate how including it would lead to differences between the two numerical models considered. Increased basal sliding leads to enhanced spatial transmission of stress gradients [*Gudmundsson*, 2003]. Since the SIA model does not account for the effects of horizontal stress transmission, this suggests that model-dependent differences will become increasingly important as the slip ratio (ratio between mean sliding and mean deformational velocity) becomes larger. For alpine glaciers a moderate slip ratio of about 1 seems to be a typical value [*Gudmundsson et al.*, 1999; *Gudmundsson*, 2003]. For Haut Glacier d'Arolla (Switzerland), *Pattyn* [2002] finds that introducing basal sliding does not lead to any significant differences between a higher-order and a zero-order model for the one particular glacier geometry studied. *Pattyn* [2002] used an altitude-independent mass balance distribution, and for that reason, no differences in steady state glacier lengths were to be expected.

[66] For any calculation of the reaction of glaciers to changes in climate a model describing the rate of mass exchange at the surface is needed in addition to a model describing the mechanics of glacier flow. Given the insignificant differences between the two mechanical models with regard to rates of advance and retreat, the question now arises if the description of glacier mechanics is less important than the description of mass balance.

[67] A way of giving a precise meaning to this question is to consider whether the rheological parameters of one of the models could possibly be changed in such a way as to make the predictions of that model identical to those of the other. If that can be done, the simpler model of the two (SIA model) will lead to predictions just as accurate as the more complex one (full-system model), and there is no need to introduce the additional level of complexity. This would, however, imply that the rheological parameters become model-dependent quantities, in which case their values will no longer reflect the true rheology of glacier ice. This is clearly a drawback, but given the way numerical models are, in practice, currently tuned, this is not a major concern.

[68] We could also ask what changes in ELA are needed to produce the observed model-dependent changes in glacier lengths. Both the rate factor $A = 2 \times 10^{-24}$ s^{-1} Pa^{-3} and ELA = 2801 m were changed by amounts of ΔA or ΔELA needed for the SIA model to reach the same steady state length as the full-system model. The required change in the flow parameter ΔA is approximately -58.5% (-1.17×10^{-24} s^{-1} Pa^{-3}) for the small, -12.5% (-0.25×10^{-24} s^{-1} Pa^{-3}) for the medium-sized, and -8.5% (-0.17×10^{-24} s^{-1} Pa^{-3}) for the large glacier. The shift ΔELA is approximately -8 m for the small, -3.2 m for the medium-sized, and -3.6 m for the large glacier. Given the uncertainties in estimated values for the rate factor for temperate ice (factor of 2–3), typical uncertainties in determination of ELA (tens of meters), and the annual natural fluctuation of ELA (on the order of hundreds of meters), these numbers allow us to conclude that the uncertainty in the rate factor, and especially the uncertainty in the mass balance, are much larger than the uncertainties introduced by the model assumptions. This supports the conclusion of *Greuell* [1992] that steady state simulations of real glaciers are expected to suffer more from the uncertainty in surface mass balance than from the assumptions of the flow model [e.g., *Oerlemans*, 2001].

[69] Although the aspect ratios (δ) of glaciers are considerably larger than for ice sheets, the effects of horizontal stress transmission on the frontal advance speed of glaciers are small. The transient evolution of small-scale features (comparable to or smaller than mean thickness) are, on the other hand, significantly different in these two models. *Gudmundsson* [2003] showed that at short spatial scales the decay times of both models differ by several orders of magnitude, with the SIA model giving too short estimates for the decay timescale. This difference in the decay times is reflected in the model-dependent response in volume and front positions following a spatially confined perturbation in mass balance over a limited period of time (Figure 11). The slower short-scale relaxation in the full-system model is the main reason why the upper-right corners of the rectangular blocks decay so much more slowly in the full-system model than in the SIA model (Figure 1).

5. Conclusions

[70] Length fluctuations of alpine glaciers over timescales of more than a few years can be modeled with sufficient accuracy using the SIA approximation. There is no need to resort to higher-order or full-system models for this purpose. Differences in response times calculated with a SIA and a full-system model are on the order of a few years. As expected, including mass balance altitude feedback increases response times, but response times for both advance and retreat remain on the order of decades to hundreds of years. Recent analytical models seem to overestimate the effect of mass balance altitude feedback on response times.

[71] **Acknowledgments.** The manuscript benefited significantly from thoughtful reviews by C. F. Raymond, an anonymous reviewer, and the Editor, R. S. Anderson, and from comments made by R. C. A. Hindmarsh, A. Jenkins, and A. Vieli. This work was supported by the ETH internal research grant number RH-11/99-2.

References

Aðalgeirsdóttir, G., G. H. Gudmundsson, and H. Björnsson (2000), The response of a glacier to a surface disturbance: A case study on Vatnajökull ice cap, *Ann. Glaciol.*, *31*, 104–110.

Albrecht, O., P. Jansson, and H. Blatter (2000), Modelling glacier response to measured mass balance forcing, *Ann. Glaciol.*, *31*, 91–96.

Elsberg, D. H., W. D. Harrison, K. A. Echelmeyer, and R. M. Krimmel (2001), Quantifying the effects of climate and surface change on glacier mass balance, *J. Glaciol.*, *47*(159), 649–658.

Glen, J. W. (1955), The creep of polycrystalline ice, *Proc. R. Soc. London, Ser. A*, *228*(1175), 519–538.

Greuell, W. (1992), Hintereisferner, Austria: Mass-balance reconstruction and numerical modelling of the historical length variations, *J. Glaciol.*, *38*(129), 233–244.

Gudmundsson, G. H. (1997), Basal-flow characteristics of a linear flow sliding frictionless over small bedrock undulations, *J. Glaciol.*, *43*(143), 71–79.

Gudmundsson, G. H. (1999), A three-dimensional numerical model of the confluence area of Unteraargletscher, Bernese Alps, Switzerland, *J. Glaciol.*, *45*(150), 219–230.

Gudmundsson, G. H. (2003), Transmission of basal variability to a glacier surface, *J. Geophys. Res.*, *108*(B5), 2253, doi:10.1029/2002JB002107.

Gudmundsson, G. H., A. Bauder, M. Lüthi, U. H. Fischer, and M. Funk (1999), Estimating rates of basal motion and internal ice deformation from continuous tilt measurements, *Ann. Glaciol.*, *28*, 247–252.

Haeberli, W., and M. Beniston (1998), Climate change and its impact on glaciers and permafrost in the Alps, *Ambio*, *27*(4), 258–265.

Halfar, P. (1981), On the dynamics of the ice sheets, *J. Geophys. Res.*, *86*(C11), 11,065–11,072.

Harrison, W. D., D. H. Elsberg, K. A. Echelmeyer, and R. M. Krimmel (2001), On the characterization of glacier response by a single time-scale, *J. Glaciol.*, *47*(159), 659–664.

Herren, E., and M. Hoelzle (1991), The Swiss glaciers, *Glaciol. Rep. 113/114–119/120*, Vers. für Wasserbau Hydrol. und Glaziol. der ETH Zürich, Switzerland.

Herren, E., M. Hoelzle, and M. Maisch (1999), The Swiss glaciers, 1995/96 and 1996/97, *Glaciol. Rep. 117/118*, Vers. für Wasserbau Hydrol. und Glaziol. der ETH Zürich, Switzerland.

Hindmarsh, R. C. A. (1990), Time-scales and degrees of freedom operating in the evolution of continental ice-sheets, *Trans. R. Soc. Edinburgh Earth Sci.*, *81*, 371–384.

Hindmarsh, R. C. A., and A. J. Payne (1996), Time-step limits for stable solutions of the ice sheet equation, *Ann. Glaciol.*, *23*, 74–85.

Hulbe, C. L., and A. J. Payne (2001), The contribution of numerical modelling to our understanding of the West Antarctic Ice Sheet, in *The West Antarctic Ice Sheet: Behavior and Environment*, *Antarct. Res. Ser.*, vol. 77, edited by R. B. Alley and R. A. Bindschadler, pp. 201–219, AGU, Washington, D. C.

Hutter, K. (1983), *Theoretical Glaciology: Material Science of Ice and the Mechanics of Glaciers and Ice Sheets*, D. Reidel, Norwell, Mass.

Huybrechts, P. (1992), The Antarctic Ice Sheet and environmental change: A three-dimensional modelling study, *Ber. Polarforsch.*, *99*, 1–241.

Jóhannesson, T. (1997), The response of two Icelandic glaciers to climatic warming computed with a degree-day glacier mass-balance model coupled to a dynamic glacier model, *J. Glaciol.*, *43*(144), 321–327.

Jóhannesson, T., C. F. Raymond, and E. D. Waddington (1989a), A simple method for determining the response time of glaciers, in *Glacier Fluctuations and Climate Change*, edited by J. Oerlemans, pp. 343–352, Kluwer Acad., Norwell, Mass.

Jóhannesson, T., C. F. Raymond, and E. D. Waddington (1989b), Timescale for adjustment of glaciers to changes in mass balance, *J. Glaciol.*, *35*(121), 355–369.

Lam, J. K.-W., and J. A. Dowdeswell (1996), An adaptive-grid finite-volume model of glacier-terminus fluctuations, *Ann. Glaciol.*, *23*, 86–93.

Leysinger, G. J.-M. C., and G. H. Gudmundsson (2000), Are higher-order numerical models needed for the analysis of rock glacier mechanics?, *Eos Trans. AGU*, *81*(48), Fall Meet. Suppl., F438.

Müller, F., T. Caflisch. and G. Müller (1976), Firn und Eis der Schweizer Alpen: Gletscherinventar, *Tech. Rep. 57*, Geogr. Inst. der ETH Zürich, Switzerland.

Nye, J. F. (1960), The response of glaciers and ice-sheets to seasonal and climatic changes, *Proc. R. Soc. London, Ser. A*, *256*(1287), 559–584.

Nye, J. F. (2000), A flow model for the polar caps of Mars, *J. Glaciol.*, *46*(154), 438–444.

Oerlemans, J. (1989), On the response of valley glaciers to climatic change, in *Glacier Fluctuations and Climate Change*, edited by J. Oerlemans, pp. 353–371, Kluwer Acad., Norwell, Mass.

Oerlemans, J. (2001), *Glaciers and Climate Change*, A. A. Balkema, Brookfield, Vt.

Pattyn, F. (2002), Transient glacier response with a higher-order numerical ice-flow model, *J. Glaciol.*, *48*(162), 467–477.

Raymond, C. F., E. D. Waddington, and T. Jóhannesson (1989), Changes in glacier length induced by climate change (abstract), *Ann. Glaciol.*, *14*, 355.

Raymond, M., G. H. Gudmundsson, and M. Funk (2003), Non-linear finite-amplitude transfer of basal perturbations to a glacier surface (abstract), in *Geophysical Research Abstracts*, vol. 5, Eur. Geophys. Soc., Nice, France.

Schmeits, M. J., and J. Oerlemans (1997), Simulation of the historical variations in length of Unterer Grindelwaldgletscher, Switzerland, *J. Glaciol.*, *43*(143), 152–164.

Steinemann, S. (1958), *Experimentelle Untersuchungen zur Plastizität von Eis*, *Geotech. Ser.*, vol. 10, Beitr. zur Geol. der Schweiz, Kümmerly and Frey, Bern.

Van der Veen, C. J. (1999), *Fundamentals of Glacier Dynamics*, A. A. Balkema, Brookfield, Vt.

Vieli, A., M. Funk, and H. Blatter (2001), Flow dynamics of tidewater glaciers: A numerical modelling approach, *J. Glaciol.*, *47*(159), 595–606.

G. H. Gudmundsson, British Antarctic Survey, Natural Environment Research Council, Madingley Road, Cambridge CB3 0ET, UK. (ghg@bas.ac.uk)

G. J.-M. C. Leysinger Vieli, Bristol Glaciology Centre, School of Geographical Sciences, University of Bristol Bristol BS8 1SS, UK. (g.leysinger-vieli@bristol.ac.uk)